bnhcrc.com.au

LARGE-EDDY SIMULATIONS OF PYRO-CONVECTION AND ITS SENSITIVITY TO ENVIRONMENTAL CONDITIONS

Research proceedings for the Bushfire and Natural Hazards CRC & AFAC conference
Adelaide, 1-3 September 2015

William Thurston, Kevin J. Tory, Robert J. B. Fawcett and Jeffrey D. Kepert
Bureau of Meteorology
Bushfire and Natural Hazards CRC

Corresponding author: w.thurston@bom.gov.au

Version	Release history	Date
1.0	Initial release of document	03/09/2015

Australian Government
Department of Industry and Science
Business
Cooperative Research
Centres Programme

Publisher:
Bushfire and Natural Hazards CRC

September 2015

Cover: A cumulonimbus cloud forms as a result of pyro-convection in the Grampians, Victoria, in 2014.

Photo by CFA Communities and Communication.

TABLE OF CONTENTS

ABSTRACT

LARGE-EDDY SIMULATIONS OF PYRO-CONVECTION AND ITS SENSITIVITY TO ENVIRONMENTAL CONDITIONS

Intense heating by a bushfire causes air to ascend, which if deep enough can cause the formation of cumulus or cumulonimbus clouds. This moist pyro-convection can potentially have a significant impact on fire behaviour by amplifying burn and spread rates, enhancing spotting through plume intensification and igniting new fires via pyrocumulonimbus lightning. Here we use large-eddy simulations to investigate the generation of pyro-convection by bushfire plumes and the sensitivity of this pyro-convection to fire intensity and environmental moisture. Moister background atmospheres produce larger, more intense pyro-convective clouds and if the background atmosphere is moist enough, intense fires can produce pyro-convection even in the absence of any moisture from the combustion. Updrafts within the simulated pyro-convection are well in excess of the fall velocities of typical firebrands and exceed those in the cases where pyro-convection does not occur. The formation of precipitation within the most intense pyro-convective clouds leads to the development of downbursts that cause strong and highly variable winds at the surface. These strong updrafts and downbursts can have significant impacts on fire behaviour.

INTRODUCTION

Intense heating of air in the vicinity of a bushfire leads to deep ascent. If this ascent is deep enough to lift air above the lifting condensation level, cumulus or cumulonimbus clouds form in a process known as moist pyro-convection. There is abundant anecdotal evidence to suggest that pyro-convective clouds may have a significant impact on fire behaviour by (i) amplifying burn and spread rates (Fromm et al., 2006; Trentmann et al., 2006; Rosenfeld et al., 2007; Fromm et al., 2012); (ii) enhancing spotting through plume intensification (Koo et al., 2010); and (iii) igniting new fires via pyrocumulonimbus lightning, noting that pyrocumulonimbus lightning conditions favour hotter and longer-lived lightning strikes (Rudlosky and Fuelberg, 2011). Pyro-convective clouds are also responsible for the transport of smoke and other aerosols into the stratosphere, resulting in hemisphere-scale smoke distribution and substantial climate impacts (Fromm et al., 2010). Therefore a knowledge of the processes that lead to the generation of moist pyro-convection is an important component of being able to understand and predict fire behaviour, as well as the potential climatic influences of large fires.

Ideal conditions for the formation of pyro-convection are similar to ideal thunderstorm conditions, but with a dry rather than moist lower troposphere (e.g. Goens and Andrews, 1998; Trentmann et al., 2006; Rosenfeld et al., 2007; Cunningham and Reeder, 2009; Fromm et al., 2012; Johnson et al., 2014). Meteorologists assess the potential of the atmosphere to generate thunderstorms in terms of its thermodynamic profile, specifically the vertical profile of air temperature and moisture. An adjustment from a thunderstorm-friendly thermodynamic profile to a fire-friendly thermodynamic profile yields the classic inverted-V profile on a thermodynamic diagram, which is also widely recognised to favour severe weather (e.g. Beebe, 1955; Wakimoto, 1985). This profile represents a dry well-mixed lower layer over-laid by a moist middle troposphere. Profiles representative of this are present in all studies of moist pyro-convection studies that we are aware of, which suggests it may be a necessary condition for pyro-convective cloud formation. Here the dry adiabatic temperature trace forms the right side of the inverted-V, while the moisture profile, relatively dry at the surface with decreasing dew-point depression to near-saturation in the middle troposphere, makes up the left side.

The inverted-V profile also favours downburst development, when precipitation from the moist middle-troposphere evaporates as it falls through the dry layer below, extracting latent heat from the air and cooling it. If precipitation does develop in pyro-convective clouds, downbursts should therefore be expected (Rothermel, 1991). These downbursts can be very hazardous to fire crews as the winds can be gusty and intense and come from a direction completely different from the ambient flow, and in complex terrain may further accelerate down valleys causing highly unpredictable changes in fire intensity and spread, as occurred in the Dude River (Arizona, USA) fire in which six fire fighters perished, (Goens and Andrews, 1998). Moreover, downburst winds are much more difficult to predict than other common causes of wind change, increasing the danger to fire crews.

It was noted above that the heat from the fire provides the lifting mechanism to initiate cumulus formation in pyro-convection. The other necessary ingredient is sufficient moisture, which when condensed produces latent heating that enhances the plume buoyancy. There are three potential sources of moisture in a bushfire plume: (i) environmental air drawn into the fire and entrained into the plume; (ii) moisture in the fuels evaporated by the intense heat of the fire; and (iii) the moisture released as the by-product of cellulose combustion (Potter, 2005). Although moisture is known to be important for the generation of pyro-convection, there is still considerable uncertainty about the relative importance of moisture from the environment versus moisture from the fire. For example, two recent case studies are at odds: Trentmann et al. (2006) find that moisture from the fire is not important for the generation of pyro-convection, whereas Cunningham and Reeder (2009) conclude that it is essential.

In this study we use large-eddy simulations to investigate the potential for the generation of moist pyro-convection by bushfire plumes. Simulations are performed for a range of (i) fire intensities and (ii) environmental moisture levels. In cases in which pyro-convective clouds are found to form, their sensitivity to the environmental conditions is explored.

METHODOLOGY

Idealised simulations of bushfire plumes are performed using a cloud-resolving model, the UK Met Office Large-Eddy Model (LEM) described by Gray et al. (2001). The model configuration used here for simulating bushfire plumes with the LEM is described in Thurston et al. (2013), with some modifications as follows. The main change made is the inclusion of moist processes within the model, necessary for the simulation of pyro-convection. The model includes a three-phase microphysics scheme (Swann, 1998), which calculates the phase changes between the vapour, liquid and frozen water species. The domain top is also raised to 12.7 km to allow the vertical growth of pyrocumulus, which may have been restricted in our previous simulations.

The model is initialised with a potential temperature profile consisting of a 4.0 km deep well-mixed layer, of a constant value of 310 K, and a stably stratified troposphere with a gradient of 3.0 K km^{-1} above the mixed layer. The initial water vapour mixing ratio profile is specified as a constant value throughout the 4.0 km deep well-mixed layer, and is then reduced above the mixed-layer top at a rate such that the relative humidity remains constant throughout the troposphere. These conditions are representative of those associated with high fire-danger conditions: there is a deep, well-mixed boundary layer and the temperature and dew point profiles plotted on a skew-T log-p diagram together form a classic inverted-V (Figure 1). The model is initialised with no background horizontal wind, allowing us to concentrate on the effects of the thermodynamics on pyro-convective cloud formation.

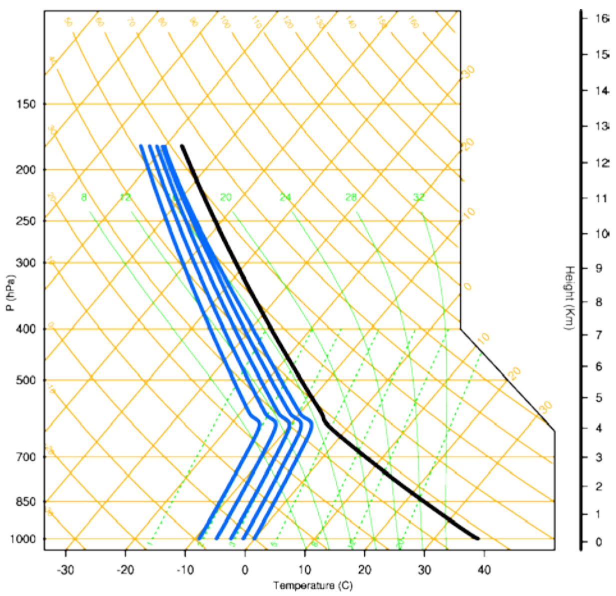

FIGURE 1: SKEW-T LOG-p DIAGRAM OF THE BACKGROUND ATMOSPHERIC CONDITIONS BEFORE THE INTENSE SURFACE HEATING IS RAMPED UP. ALL SIMULATIONS HAVE THE SAME TEMPERATURE PROFILE, SHOWN IN BLACK, AND THE FIVE DIFFERENT DEW-POINT PROFILES ARE SHOWN IN BLUE.

A range of simulations is performed here, in order to explore the sensitivity of the formation of pyro-convection to (i) the background moisture and (ii) fire intensity. Five sets of initial conditions for the simulation of bushfire plumes are created by initialising the model as described above, with five different values for the (constant) mixed-layer water vapour mixing ratio, q_v, of 2.0, 2.5, 3.0, 3.5 and 4.0 g kg^{-1}. The resultant five sets of initial conditions are shown in Figure 1. Bushfire plumes are then generated by imposing a localised intense heat flux at the model surface over a circular area of radius 250 m, centred at (x, y) = (0.0, 0.0) km. Four different fire intensities, Q, of 5, 10, 20 and 30 kW m^{-2} are simulated and in each case the heat flux is linearly ramped up from zero to its peak value over five minutes, then held constant for one hour, before being linearly ramped down back to zero over five minutes. The combination of five background moisture profiles and four bushfire intensities gives us twenty different simulations in total. In the simulations presented here there is no representation of the moisture flux from the fire, either from moisture within the fuels or from the combustion process itself.

RESULTS

Figure 2 shows a snapshot from the Q = 30 kW m^{-2} fire intensity and q_v = 4.0 g kg^{-1} boundary-layer water vapour mixing ratio simulation, 22 minutes after the fire has reached maximum intensity. This is the simulation with the moistest background conditions and the highest fire intensity. The bushfire plume has a strong updraft throughout most of the extent of the boundary layer, with a maximum vertical velocity in excess of 25 m s^{-1} (Figure 2 (a)). The plume decelerates as it penetrates into the stably stratified troposphere, but the ascent is deep enough to trigger the formation of a pyrocumulus cloud. The cloud base is located at 4.5 km above ground level (AGL) and the cloud extends to an altitude of 7.5 km AGL (Figure 2 (c)). Although the bushfire updraft core is relatively slender within the boundary layer, the horizontal extent of the pyrocumulus cloud is much greater, having a diameter in excess of 3 km (Figure 2 (d)). Extensive condensation within the cloud, notable in the liquid water mixing ratio field around (x,z) = (0.5,6.5) km, leads to the release of latent heat which is evident in the potential temperature perturbation field at the same location (Figure 2 (b)). There is a co-located updraft greater than 10 m s^{-1} within the pyrocumulus cloud, which is separated from the main plume updraft within the boundary layer. This resurgence of the updraft is due to latent heat release increasing the local plume buoyancy.

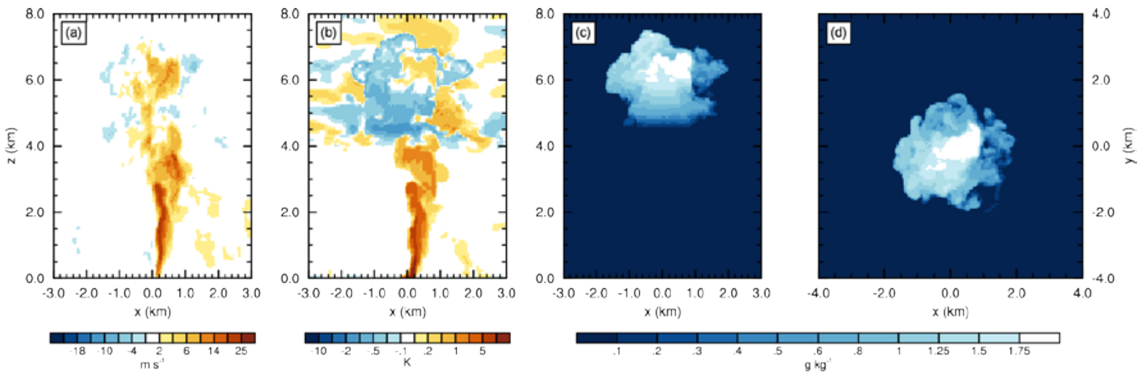

FIGURE 2: VERTICAL CROSS-SECTIONS OF THE INSTANTANEOUS (A) PLUME VERTICAL VELOCITY, M S^{-1}, AND (B) PLUME POTENTIAL TEMPERATURE PERTURBATION, K, BOTH IN THE Y = 0 PLANE. INSTANTANEOUS LIQUID WATER MIXING RATIO, G KG^{-1}, MAXIMUM VALUES IN THE (C) Y– AND (D) Z–DIRECTIONS. ALL PLOTS ARE SHOWN AT 22 MINUTES AFTER THE FIRE HAS REACHED FULL INTENSITY AND ARE FOR THE Q = 30 KW M^{-2} FIRE INTENSITY AND q_v = 4.0 G KG^{-1} BOUNDARY-LAYER WATER VAPOUR MIXING RATIO CASE.

The pyro-convection in this case is intense enough for substantial precipitation to begin forming approximately 22 minutes after the fire has reached maximum intensity. As the precipitation falls from the relatively moist troposphere through the warmer and drier lower levels of the atmosphere it evaporates, cooling the air. This negatively buoyant air then accelerates towards the surface in a downdraft. It should be noted that downdrafts are only found in this simulation and the Q = 30 kW m^{-2}, q_v = 3.5 g kg^{-1} simulation, in which the atmosphere is slightly drier.

Figure 3 shows vertical cross-sections at three stages of the downdraft development, positioned approximately through the centre of the downdraft and focused on the lowest 2 km of the atmosphere. When the downdraft has descended just far enough to touch the surface at 44.5 minutes after the fire has reached full intensity, Figure 3 (a), the main core of the downdraft is at about 1.2 km AGL, denoted by marker α, and has an intensity in excess of -8 m s^{-1}. A secondary, weaker, downdraft core closer to the surface is denoted by marker β at about 0.2 km AGL. At 53.5 minutes after the fire has reached full intensity, Figure 3 (b), the downburst has impacted on the surface and begun to spread out laterally in both directions as a gust front. The downdraft has split, with the core previously labelled α spreading to the left and the core previously labelled β spreading to the right. A vertical velocity couplet is visible at each leading edge of the gust front, with an updraft ahead of the leading edge and descending motion immediately behind it. These couplets are labelled γ in Figure 3 (b). At this time the downdraft core has become larger and less uniform, covering the region denoted by marker δ, with an intensity now in excess of -9 m s^{-1}. By 61.0 minutes after the fire has reached full intensity, Figure 3 (c), the downdraft is orientated slantwise and the intensity has decreased to approximately -6 m s^{-1}.

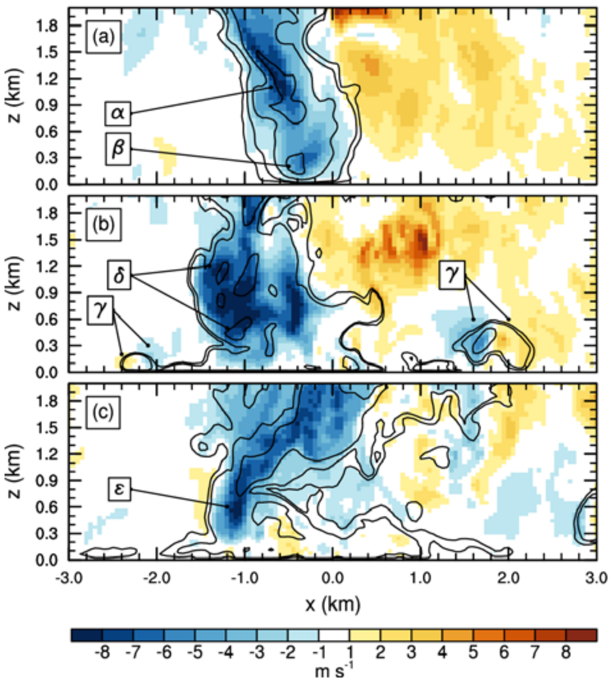

FIGURE 3: VERTICAL CROSS-SECTIONS OF THE PYRO-CONVECTIVELY GENERATED DOWNDRAFT IN THE Y = 0.65 KM PLANE AT (A) 44.5, (B) 53.5 AND (C) 61.0 MINUTES AFTER THE Q = 30 KW M^{-2} FIRE HAS REACHED FULL INTENSITY IN THE q_v = 4.0 G KG^{-1} BOUNDARY-LAYER WATER VAPOUR MIXING RATIO CASE. THE VERTICAL VELOCITY, M S^{-1}, IS SHOWN IN FILLED COLOUR AND THE POTENTIAL TEMPERATURE PERTURBATION CONTOUR LINES OF Θ = -0.1,-0.2,-0.5 AND -1.0 K ARE OVERLAID.

The near-surface effects of the downburst and associated gust front are illustrated by the plan views and time series of the 10-m wind speed shown in Figure 4. At 52.0 minutes after the fire has reached full intensity, Figure 4 (a), the gust front is expanding out laterally in all directions with the maximum 10-m wind speeds found in a ring around the leading edge. The gust front currently passing through the time-series location (denoted by the black diamond) originated from the core labelled by marker α in Figure 3 (a) at 44.5 minutes after the fire has reached full intensity. Four minutes later a second downdraft core has impacted upon the surface and begun to spread as a gust front laterally through the time-series location with a peak wind speed in excess of 11 m s^{-1} (40 km h^{-1}), Figure 4 (b), followed just two minutes later by a third gust front, Figure 4 (c). The origin of these two gust fronts is hard to separate and they both come from the region labelled by marker δ in Figure 3 (b). Gust fronts continue to pass through the time-series location (e.g. Figure 4 (d) but they begin to become less coherent. The time-series plot, Figure 4 (e), clearly illustrates the intensity and the large variability of the near-surface wind wind speeds as each gust front passes through the time-series location. Six gusts in excess of 8 m s^{-1} (29 km h^{-1}), separated by calmer conditions, occur in the space of about 15 minutes.

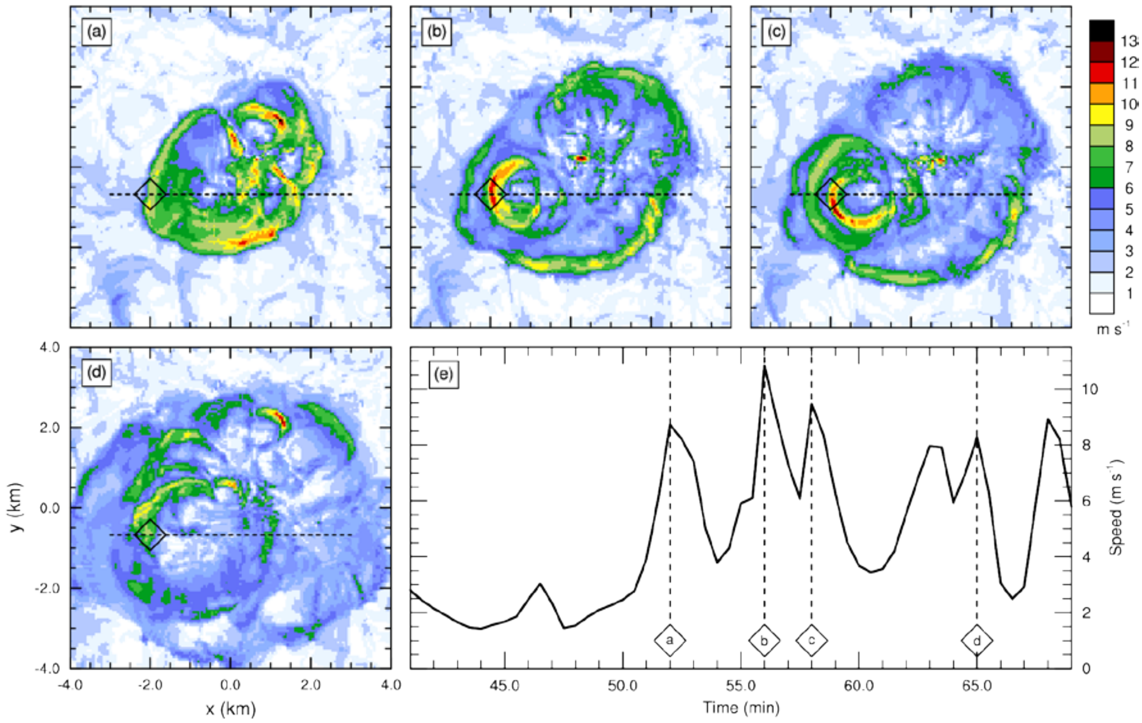

FIGURE 4: PLAN VIEWS OF THE INSTANTANEOUS 10-M WIND SPEED, M S^{-1}, AT (A) 52, (B) 56, (C) 58 AND (D) 65 MINUTES AFTER THE Q = 30 KW M^{-2} FIRE HAS REACHED FULL INTENSITY IN THE q_v = 4.0 G KG^{-1} BOUNDARY-LAYER WATER VAPOUR MIXING RATIO CASE. THE BLACK DIAMOND OVERLAID ON EACH OF THE PANELS (A)–(D) DENOTES THE LOCATION OF THE 10-M WIND SPEED TIME SERIES, M S^{-1}, SHOWN IN PANEL (E) AND THE HORIZONTAL DASHED LINE DENOTES THE LOCATION OF THE VERTICAL CROSS-SECTIONS SHOWN IN FIGURE 3.

Figure 5 shows a snapshot of the liquid water mixing ratio vertical cross-sections for all twenty combinations of Q and q_v, at 22 minutes after the fires have reached full intensity. The potential formation of a pyrocumulus cloud and the properties of that cloud are dependent on both the intensity of the fire and the environmental moisture. Pyrocumulus is more likely to form if the environment is moist and the fire intensity is high. The size of a pyrocumulus and its cloud top height both increase with environmental moisture and fire intensity. In the driest environment, with a boundary-layer water vapour mixing ratio of 2.0 g kg^{-1}, pyrocumulus only forms for the most intense fire and the cloud that does form is very small. As the environmental moisture increases, pyrocumulus forms for weaker and weaker fire intensity, and by the time the boundary-layer water vapour mixing ratio reaches the maximum value of 4.0 g kg^{-1}, pyrocumulus forms for all values of fire intensity. For a fixed fire intensity, increasing the boundary-layer water vapour mixing ratio lowers the cloud-base height, from 5.7 km AGL for the driest to 4.5 km AGL for the moistest. Conversely for a fixed boundary-layer water vapour mixing ratio, increasing the fire intensity does not substantially affect cloud-base height.

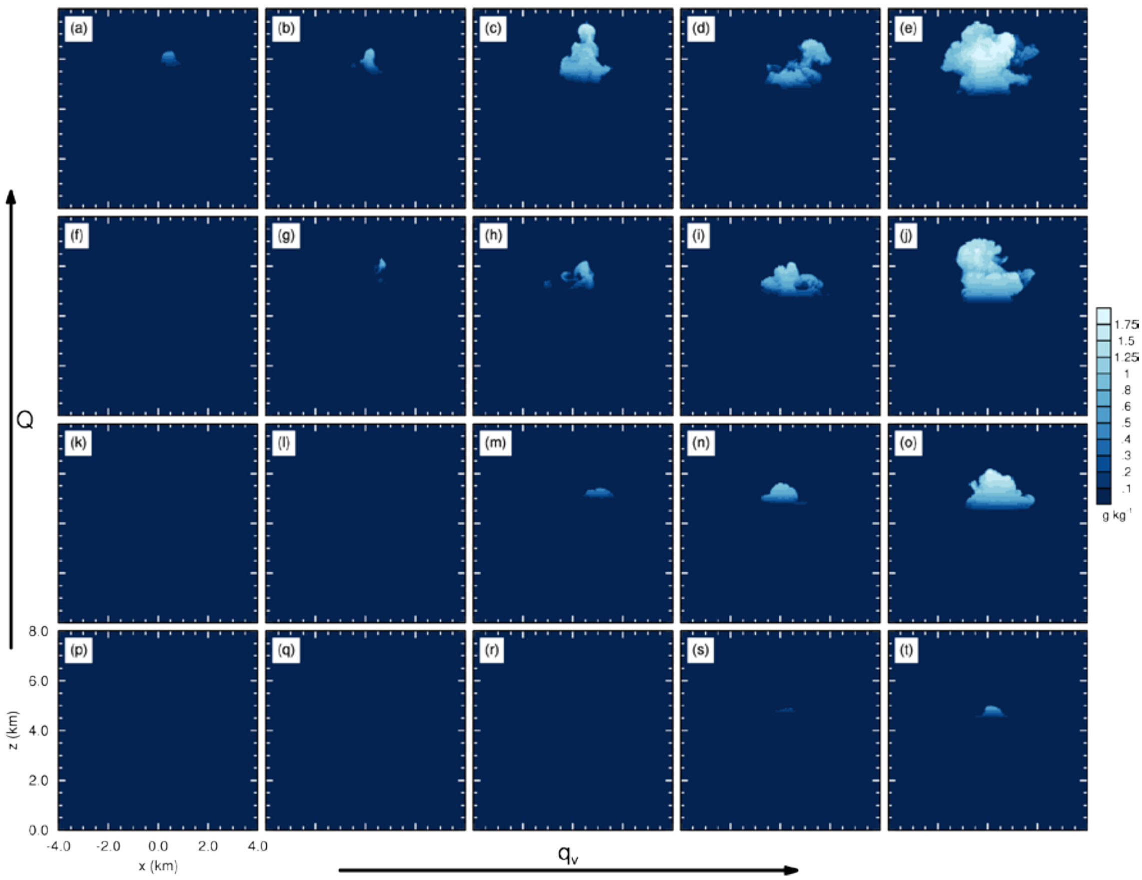

FIGURE 5: VERTICAL CROSS-SECTIONS OF THE MAXIMUM INSTANTANEOUS LIQUID WATER MIXING RATIO IN THE *Y*–DIRECTION, G KG^{-1}, AT 22 MINUTES AFTER THE FIRES HAVE REACHED FULL INTENSITY. PANELS SHOW ALL TWENTY COMBINATIONS OF FIRE INTENSITY, Q = (5,10,20,30) KW M^{-2}, ARRANGED VERTICALLY AND BOUNDARY-LAYER WATER VAPOUR MIXING RATIO, q_v = (2.0, 2.5, 3.0, 3.5, 4.0) G KG^{-1}, ARRANGED HORIZONTALLY. FIRE INTENSITY INCREASES FROM THE BOTTOM ROW OF PANELS TO THE TOP ROW OF PANELS AND BOUNDARY-LAYER WATER VAPOUR MIXING RATIO INCREASES FROM THE LEFT-HAND COLUMN OF PANELS TO THE RIGHT-HAND COLUMN OF PANELS, AS INDICATED BY THE ARROWS.

SUMMARY AND DISCUSSION

Large-eddy simulations of bushfire plumes have been performed in background atmospheric conditions representative of high fire-danger days. The potential for the formation of pyro-convection has been investigated by varying the environmental moisture and the fire intensity. Intense fires in moist atmospheres formed larger pyrocumulus than weak fires in dry atmospheres, which in some cases formed no pyrocumulus at all. Increasing the environmental moisture reduced the cloud-base height, whereas increasing the fire intensity had no discernible effect on cloud-base height. The pyro-convection generated by the most intense fire and in the moistest environmental conditions was strong enough for the formation of substantial precipitation, which subsequently led to the formation of evaporatively-cooled downdrafts. As the downdrafts impacted upon the surface they spread laterally as a series of concentric gust fronts, with peak 10-m wind speeds in excess of 11 m s^{-1} found in the strongest gust front.

There are two mechanisms identifiable in these simulations through which pyro-convection has potential to have a significant impact of fire behaviour. Firstly, the resurgence of the plume updraft due to the latent heat released within a pyrocumulus has the potential to increase the height to which firebrands are lofted, particularly as the pyrocumulus updrafts are in excess of 10 m s^{-1}, considerably greater than the fall velocity of typical firebrands of 4–6 m s^{-1} (e.g. Ellis, 2010). Lofting the firebrands higher into the atmosphere has the potential to then increase the distance they travel before landing, although detailed calculations similar to those performed by Thurston et al. (2014) would need to be performed to accurately assess the potential impact of pyro-convection on spotting distance. Secondly, the formation of downdrafts and their associated gust fronts has implications for the surface-based fire spread. The sudden increase in wind speed as the gust front passes will increase burn and spread rates, but there is also a large amount of speed and direction variability associated with the downburst. The downburst is seen to comprise multiple cores impacting the surface, resulting in many gust fronts spreading out in concentric rings. This variability is not captured within the traditional conceptual model of a pool of cold air descending then spreading out radially and means that if fire fighters on the ground experience the passage of a gust front, they should be prepared for gusty variable conditions to continue for some time. In the case presented here six surface gusts in excess of 8 m s^{-1}, all separated by calmer conditions, were experienced over the space of 15 minutes. Although we are currently unable to forecast the precise location and timing of an individual pyro-convective updraft or downburst, by performing studies such as this we are able to learn about the conditions under which they form, their dynamics and potential impact on fire behaviour. Future work will use a similar framework to systematically explore the relative importance of moisture from the environment and moisture released in the combustion process for the generation on pyro-convective clouds.

ACKNOWLEDGEMENTS

We thank the UK Met Office for the provision of their Large Eddy Model code. Andrew Dowdy, Chris Lucas and two anonymous reviewers are thanked for their comments on an earlier version of this manuscript. This research was undertaken with the assistance of resources from the National Computational Infrastructure (NCI), which is supported by the Australian Government.

REFERENCES

1 Beebe, R. G., 1955: Types of airmasses in which tornadoes occur. *B. Am. Meteorol. Soc.,* **36,** 349–350.

2 Cunningham, P. and M. J. Reeder, 2009: Severe convective storms initiated by intense wildfires: Numerical simulations of pyro-convection and pyro-tornadogenesis. *Geophys. Res. Lett.,* **36,** L12812, 10.1029/2009GL039262.

3 Ellis, P. F. M., 2010: The effect of the aerodynamic behaviour of flakes of jarrah and karri bark on their potential as firebrands. *J. Roy. Soc. West. Aust.,* **93,** 21–27.

4 Fromm, M., D. T. Lindsey, R. Servranckx, G. Yue, T. Trickl, R. Sica, P. Doucet, and S. Godin-Beekmann, 2010: The untold story of pyrocumulonimbus. *B. Am. Meteorol. Soc.,* **91,** 1193–1209.

5 Fromm, M., A. Tupper, D. Rosenfeld, R. Servranckx, and R. McRae, 2006: Violent pyro-convective storm devastates Australia's capital and pollutes the stratosphere. *Geophys. Res. Lett.,* **33,** L05815, 10.1029/2005GL025161.

6 Fromm, M. D., R. H. D. McRae, J. J. Sharples, and G. P. Kablick, III, 2012: Pyrocumulonimbus pair in Wollemi and Blue Mountains National Parks, 22 November 2006. *Aust. Meteorol. Ocean J.,* **62,** 117–126.

7 Goens, D. W. and P. L. Andrews, 1998: Weather and fire behavior factors related to the 1990 Dude fire near Payson, AZ. *Proceedings of the 2nd Symposium on Fire and Forest Meteorology,* Boston, MA, American Meteorological Society, 153–158.

8 Gray, M. E. B., J. Petch, S. H. Derbyshire, A. R. Brown, A. P. Lock, H. A. Swann, and P. R. A. Brown, 2001: Version 2.3 of the Met Office large eddy model: Part II. Scientific documentation. Turbulence and Diffusion Note 276, UK Met Office, 49 pp., Exeter, United Kingdom.

9 Johnson, R. H., R. S. Schumacher, J. H. Ruppert, Jr., D. T. Lindsey, J. E. Rutherford, and L. Kriederman, 2014: The role of convective outflow in the Waldo Canyon fire. *Mon. Weather Rev.,* **142,** 3061–3080.

10 Koo, E., P. J. Pagni, D. R. Weise, and J. P. Woycheese, 2010: Firebrands and spotting ignition in large-scale fires. *Int. J. Wildland Fire,* **19,** 818–843.

11 Potter, B. E., 2005: The role of released moisture in the atmospheric dynamics associated with wildland fires. *Int. J. Wildland Fire,* **14,** 77–84.

12 Rosenfeld, D., M. Fromm, J. Trentmann, G. Luderer, M. O. Andreae, and R. Servranckx, 2007: The Chisholm firestorm: observed microstructure, precipitation and lightning activity of a pyro-cumulonimbus. *Atmos. Chem. Phys.,* **7,** 645–659.

13 Rothermel, R. C., 1991: Predicting behavior and size of crown fires in the northern Rocky Mountains. Research Paper INT-438, USDA Forest Service, 46 pp., Intermountain Research Station.

14 Rudlosky, S. D. and H. E. Fuelberg, 2011: Seasonal, regional, and storm-scale variability of cloud-to-ground lightning characteristics in Florida. *Mon. Weather Rev.,* **139,** 1826–1843.

15 Swann, H., 1998: Sensitivity to the representation of precipitating ice in CRM simulations of deep convection. *Atmos. Res.,* **47–48,** 415–435.

16 Thurston, W., K. J. Tory, R. J. B. Fawcett, and J. D. Kepert, 2013: Large-eddy simulations of bushfire plumes in the turbulent atmospheric boundary layer. *MODSIM2013, 20th International Congress on Modelling and Simulation,* J. Piantadosi, R. S. Anderssen, and J. Boland, Eds., Modelling and Simulation Society of Australia and New Zealand, 284–289, ISBN: 978-0-9872143-3-1.

17 Thurston, W., K. J. Tory, J. D. Kepert, and R. J. B. Fawcett, 2014: The effects of fire-plume dynamics on the lateral and longitudinal spread of long-range spotting. *Proceedings of the Research Forum at the Bushfire and Natural Hazards CRC & AFAC 2014 Conference,* M. Rumsewicz, Ed., Bushfire and Natural Hazards CRC, 85–94, ISBN: 978-0-9941696-3-15.

18 Trentmann, J., et al., 2006: Modeling of biomass smoke injection into the lower stratosphere by a large forest fire (Part I): reference simulation. *Atmos. Chem. Phys.,* **6,** 5247–5260.

19 Wakimoto, R. M., 1985: Forecasting dry microburst activity over the high plains. *Mon. Weather Rev.,* **113,** 1131–1143.